Efficient Syntheses of the Complete Set of Compounds $[\{(OC)_5M\}_6E_6]^{2-}$ (M = Cr, Mo, W; E = Ge, Sn) − Structure and Redox Behaviour of the Octahedral Clusters $[Ge_6]^{2-}$ and $[Sn_6]^{2-}$

Gerd Renner,[a] Peter Kircher,[a] Gottfried Huttner,*[a] Peter Rutsch,[a] and Katja Heinze[a]

Dedicated to Professor Dieter Sellmann on the occasion of his 60th birthday

Keywords: Main-group elements / Cluster compounds / Carbonyl ligands / NMR spectroscopy / Germanium / Tin

Improved syntheses of the known clusters $[\{(OC)_5Cr\}_6Ge_6]^{2-}$ (**1**) and $[\{(OC)_5Cr\}_6Sn_6]^{2-}$ (**4**) are reported. The new synthetic procedures also allow for the preparation of the molybdenum and tungsten derivatives $[\{(OC)_5M\}_6Ge_6]^{2-}$ (M = Mo: **2**; M = W: **3**) and $[\{(OC)_5M\}_6Sn_6]^{2-}$ (M = Mo: **5**; M = W: **6**). Compounds **1**–**6** were obtained as crystalline $[Ph_4P]$ salts, whose structures were determined for the whole series **1**–**6** by single-crystal X-ray analyses. All six $[Ph_4P]$ salts crystallise in tetragonal space groups, with the site group symmetries of the cluster core ranging from C_{4h} to D_{4h}. The average octahedral symmetry of the cluster core in solution is evident from ^{119}Sn NMR spectroscopic data. Reversible one-electron oxidation of the dianions is suggested by cyclovoltammograms, while reduction is irreversible throughout. Electronic transitions which could be due to the cluster core were not found in the experimentally accessible energy range above 300 nm (below 4 eV). These findings indicate a high intrinsic stability of the precise electron clusters $[Ge_6]^{2-}$ and $[Sn_6]^{2-}$.

Introduction

The main group clusters $[Sn_6]^{2-}$ and $[Ge_6]^{2-}$ have been characterised in the form of their organometallic derivatives $[\{(OC)_5Cr\}_6Sn_6]^{2-}$ (**4**) and $[\{(OC)_5Cr\}_6Ge_6]^{2-}$ (**1**).[1,2] While octahedral aggregates are a common type of arrangement for transition-metal clusters and a common motif in the structural chemistry of boranes and carboranes, they are by no way the preferred motif for the aggregation of other main-group elements, either in molecular compounds or in solid-state phases.[3] Thus anionic aggregates of the heavier group-14 elements $[E_m]^{n-}$ of tetrahedral shape e.g. $[Ge_4]^{2-}$, of trigonal-bipyramidal shape $[E_5]^{n-}$ [4,5] or of a shape somewhere between a monocapped archimedian antiprism (*nido*) and a tricapped trigonal prism (*closo*) $[E_9]^{n-}$ [6−11] are well-characterised species known as components of solid-state structures.[3,12] They are also, to a lesser extent, known in molecular anions in solution or in salt-type molecular compounds. No aggregate of the type $[E_6]^{n-}$ [13,14] has ever been observed until now, and it is only in an organometallic environment that such species are persistent in molecular anions. The compounds $[\{(OC)_5Cr\}_6Sn_6]^{2-}$ (**4**)[1] and $[\{(OC)_5Cr\}_6Ge_6]^{2-}$ (**1**)[2] are the only ones thus far characterised. Their octahedral structures are well documented,[1,2] but their chemical properties could not yet be studied in detail as they are difficult to prepare in large amounts. Analysing the properties of these prototype species would be interesting for the following reasons:

Simple MO models predict that the clusters $[E_6]^{2-}$ (E = Ge, Sn), which form the core of their organometallic derivatives $[(L_nM)_6E_6]^{2-}$ (L_nM = 16 electron transition metal template), should be especially stable in view of their large HOMO−LUMO gap. This is in agreement with the accepted electron-counting rules[15,16] which state that *closo* octahedral species are stable, with seven skeleton electron pairs which is just the number of such pairs in $[E_6]^{2-}$ (E = group-14 element). On the basis of this model, it can be deduced that oxidation as well as reduction of such species should be difficult, and reduction might well lead to rearrangements, producing more open forms of the clusters.[15,16] A large HOMO−LUMO gap, as expected on the basis of such models, would also mean that electronic absorptions arising from transitions within the cluster framework should have a relatively high energy. Furthermore, the structures of the $[E_6]^{2-}$ entities should be close to octahedral in each case, largely independent of the type of organometallic protecting group L_nM. This octahedral arrangement should also persist in solution.

With all these questions in mind, it appears necessary to search for better synthetic strategies to produce the compounds $[(L_nM)_6E_6]^{2-}$. It had recently been found that the digermanium derivative $[\{(OC)_5Cr\}_2Ge_2I_4]^{2-}$, which is itself obtained by the reduction of GeI_2 with $Na_2[Cr_2(CO)_{10}]$, is a suitable precursor from which $[\{(OC)_5Cr\}_6Ge_6]^{2-}$ (**1**) is obtained in up to 40% yield by further reduction.[17] This result stimulated a more systematic screening of the reactions of $[M_2(CO)_{10}]^{2-}$ [18,19] (M = Cr, Mo, W) with $EHal_2$ (GeI_2, $SnCl_2$). In this way, feasible procedures for the syntheses of $[\{(OC)_5M\}_6E_6]^{2-}$ (E = Ge, Sn; M = Cr, Mo, W) have been developed such that the cyclovoltammetric and spectroscopic behaviour of these

[a] Anorganisch-Chemisches Institut der Universität Heidelberg
Im Neuenheimer Feld 270, 69120 Heidelberg, Germany
Fax: (internat.) + 49-(0)6221/545707
E-mail: g.huttner@indi.aci.uni-heidelberg.de

  1434−1948/01/0404−0973 $ 17.50+.50/0

compounds, as well as their solid-state and solution structures, could now be studied in detail. The results of these preparative efforts and the spectroscopic, cyclovoltammetric, and structural studies are reported in this paper.

Results and Discussion

Preparation of Ge_6 Clusters

It had been shown that $K_2[Cr(CO)_5]$ reacts with $SnCl_2$ to produce $[\{(OC)_5Cr\}_6Sn_6]^{2-}$ (**4**) which could be isolated in the form of its $K(crypt)_2$ salt.[1] The straightforward transfer of this synthetic approach to the chemistry of germanium did, however, not result in an analogous $[\{(OC)_5Cr\}_6Ge_6]^{2-}$ cluster. Only when $Na_2[Cr_2(CO)_{10}]$ was treated with GeI_2 in the presence of bipy (bipy = 2,2′-bipyridine), did the cluster $[\{(OC)_5Cr\}_6Ge_6]^{2-}$ (**1**) result (Scheme 1), which was isolated as its Ph_4P salt.[2]

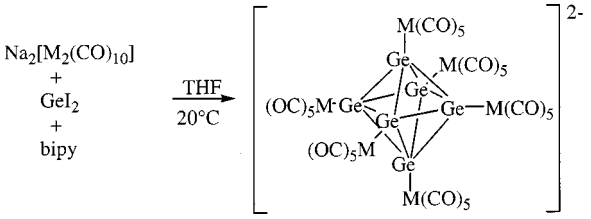

1 (M = Cr, yield: 11%)
2 (M = Mo, yield: 9%)
3 (M = W, yield: 9%)

Scheme 1. Syntheses and yields of **1**–**3** from a 1:1:1 mixture of the reagents

This type of procedure was now found to work with the decacarbonyldimetallates of molybdenum and tungsten as well, to produce **2** and **3**, respectively. The yields obtained in this route are modest throughout, with a maximum of 11% in the case of chromium and approximately 9% in the case of molybdenum and tungsten.

It has now been found that changing the stoichiometry of the reactants by increasing the amount of the dimetallate to a threefold molar excess with respect to GeI_2, produces the desired clusters in fair yields, without any addition of bipy (Scheme 2).

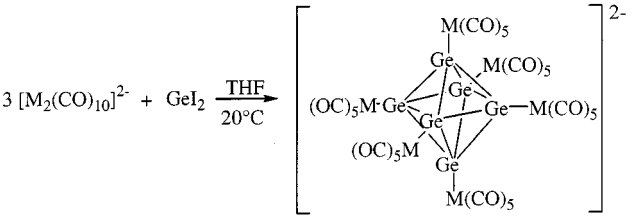

2 (M = Mo, yield: 47%)
3 (M = W, yield: 60%)

Scheme 2. Syntheses and yields of **2**, **3** from a 1:3 mixture of the reagents

It appears therefore that the only function of bipy in the reported synthesis of **1**[2] is to reduce the amount of GeI_2 by complexation, such that the stoichiometric excess of the dimetallate relative to the germanium iodide is appropriately increased.[20]

For the reaction of $[Cr_2(CO)_{10}]^{2-}$ with GeI_2, it has been shown that $[\{(OC)_5Cr\}I_2Ge-GeI_2\{Cr(CO)_5\}]^{2-}$ is obtained when the stoichiometric ratio of $[Cr_2(CO)_{10}]^{2-}$ and GeI_2 is 1:1.[17] This digermanium compound is an intermediate in the reductive pathway from GeI_2 to the $[Ge_6]^{2-}$ core of **1**: Further reduction of $[\{(OC)_5Cr\}I_2Ge-GeI_2\{Cr(CO)_5\}]^{2-}$ with 2 equiv. of $[Cr_2(CO)_{10}]^{2-}$ produces **1** in fair yields (Scheme 3).[17]

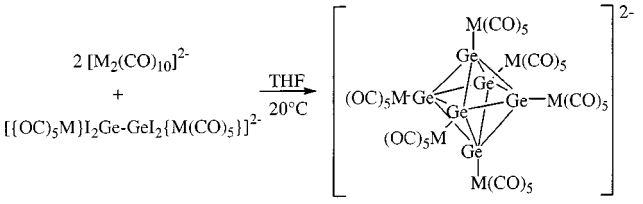

1 (M = Cr, yield: 40%)
3 (M = W, yield: 60%)

Scheme 3. Syntheses of **1** and **3** from tetraiododigermanate(2−)-precursors in a ratio 2:1

This type of reaction has been reported for compound **1**.[17] It has now been found that **3** can be obtained in good yields (60%) from $[\{(OC)_5W\}I_2Ge-GeI_2\{W(CO)_5\}]^{2-}$ [17] and 2 equiv. of $[W_2(CO)_{10}]^{2-}$. The decacarbonyldimetallates may be used as their sodium[18] or potassium salts,[19] without a significant change in reactivities and yields. The tetraiododigermanate derivatives $[\{(OC)_5M\}I_2Ge-GeI_2\{M(CO)_5\}]^{2-}$ are easily accessible for M = Cr, W, while for M = Mo the corresponding compound could not be isolated in a pure state. Its production is always accompanied by the formation of **2**, and it was not yet possible to separate the digermanate derivative from this cluster. For M = Cr and W, on the other hand, the compounds $[\{(OC)_5M\}I_2Ge-GeI_2\{M(CO)_5\}]^{2-}$ are ideal starting materials for the syntheses of **1** and **3**. Their reduction to these cluster compounds by KC_8 (Scheme 4) is a clean reaction from which the clusters are easily obtained in a pure state.

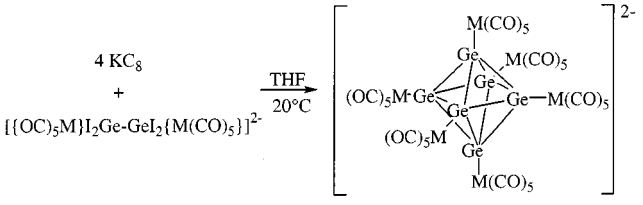

1 (M = Cr, yield: 42%)
3 (M = W, yield: 60%)

Scheme 4. Syntheses and yields of **1** and **3** by KC_8 reduction

Preparation of Sn_6 Clusters

The first compound of the series (**4**) was obtained from the reaction of $K_2[Cr(CO)_5]$ with $SnCl_2$.[1] It has now been found that the reaction of $Na_2[Cr_2(CO)_{10}]$ with $SnCl_2$ in a

1:1 molar ratio also leads to the formation of **4** (Scheme 5, Table 1).

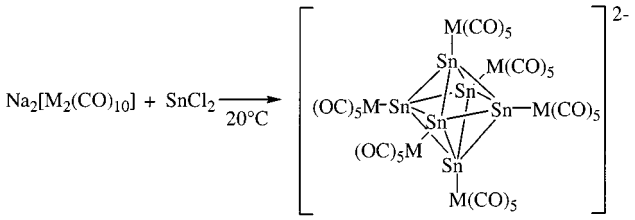

4 (M = Cr, yield: 11%)
5 (M = Mo, yield: 36%)
6 (M = W, yield: 9%)

Scheme 5. Syntheses and yields of **4**–**6**

Table 1. Complexes of type **1**–**6**

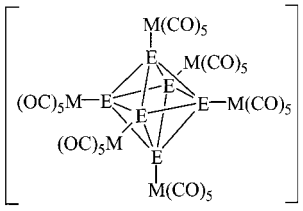

	E	M	Cation
1	Ge	Cr	$[Ph_4P^+]$
2	Ge	Mo	$[Ph_4P^+]$
3	Ge	W	$[Ph_4P^+]$
4	Sn	Cr	$[Ph_4P^+]$
5	Sn	Mo	$[Ph_4P^+]$
6	Sn	W	$[Ph_4P^+]$

The reaction is sensitive to the molar ratio of the reactants: When $Na_2[Cr_2(CO)_{10}]$ and $SnCl_2$ are used in a 3:1 ratio, the star-type compound $[Sn\{Cr(CO)_5\}_3]^{2-}$ is the main product.[21] With $Na_2[Mo_2(CO)_{10}]$ or $Na_2[W_2(CO)_{10}]$ used in the same molar ratio, mixtures of products are obtained which do not contain any **5** or **6**, as judged from their IR absorptions. When a ratio of 1:1 is used, the isolated yield of **4** (as its Ph_4P salt) is approximately 10%, along with other products in the reaction mixture. $[\{(OC)_5Cr\}SnCl_3]^-$ and $[\{(OC)_5Cr\}_2SnCl_2]^{2-}$ (both isolated as their Ph_4P salts) were found to be formed in substantial amounts ($[Ph_4P][\{(OC)_5Cr\}SnCl_3]$, 26% and $[Ph_4P]_2[\{(OC)_5Cr\}_2SnCl_2]$, 42%). The same type of reaction has already been used to synthesise $[\{(OC)_5M\}_2SnCl_2]^{2-}$ (M = Cr, Mo, W).[22,23] These compounds were, in fact, the main products from which the clusters had to be separated by chromatography. In the case of **5**, the use of ethanol as the solvent instead of THF greatly improved the yield. In this solvent, **5** is precipitated by the addition of Ph_4PCl, while the $[Ph_4P]$ salts of the by-products remain in solution. Traces of $[Ph_4P]_2[\{(OC)_5Mo\}_2SnCl_2]$, which are precipitated together with $[Ph_4P^+]_2$·**5**, are easily washed out with ethanol such that analytically pure $[Ph_4P^+]_2$·**5** is obtained in 36% yield, without the necessity of chromatographic purification.

Structures and Properties

The structures of **1** and **4** have been reported for the phosphonium salt $[Ph_4P^+]_2$·**1**[2] and for the potassium salt $[K^+(crypt)]_2$·**4**.[1] In order to unequivocally prove the constitution of the phosphonium salts **2**–**6**, the structures were determined by X-ray analysis. Crystals of the tin compounds **4**–**6** were obtained by layering THF solutions of the salts with ethanol and the germanium compounds **2** and **3** were crystallised by layering DMA (*N*,*N*-dimethylacetamide) solutions of their salts with ethanol. From the crystals obtained this way, those of **4** contain 1 equiv. of THF per formula unit as a solvate, whereas the other compounds crystallise as such. The high symmetry of the phosphonium cation (S_4) and of the cluster anions are in agreement with tetragonal space groups, which are found for the phosphonium salts of all six compounds **1**–**6** (Table 6). The phosphorus centre of the phosphonium cation occupies a special position in each case such that its crystallographic point-group symmetry is S_4. The centres of the anionic clusters are also located at special positions. Owing to steric influence, the $M(CO)_5$ moieties have to be rotated around their Sn–M or Ge–M axes in such a way that they cannot conform to an arrangement which would be symmetric with respect to the idealised mirror planes of the "octahedron" formed by the main-group elements. The tilt imposed on these groups maximally allows for D_4 symmetry. This is the crystallographic symmetry apparent for the anions in $[Ph_4P^+]_2$·**1** and $[Ph_4P^+]_2$·**2** (space group *P*4/*nnc*). The phosphonium salts of **3**, **5**, and **6** crystallise in space group *I*4/*mmm*, which implies apparent D_{4h} symmetry of the anions. This apparent symmetry is fulfilled by a statistical 1:1 disorder of each $M(CO)_5$ group over two mirror-symmetric rotational positions. The $[Ph_4P]$ salt of **4** contains 1 equiv. of THF solvate per formula unit, its space-group symmetry is *I*4/*m*, with the crystallographic site-group symmetry of the cluster corresponding to C_{4h}. Again, this symmetry, which is exact for the Sn_6 core results from the superposition of two rotational positions of the $Cr(CO)_5$ units at the C_4 axis around their Cr–Sn bonds. The crystallographically determined symmetry of the "octahedron" formed by the main-group elements corresponds to the site-group symmetry in each case, and is, in fact, D_{4h} throughout. Therefore the main-group clusters have a tetragonally distorted octahedral symmetry. The observed distortion corresponds to a slight elongation of the octahedra along the C_4 axis (Table 2, Figure 1).

As the quantitative data (Table 2) show, there is a slight variation of the Ge–Ge distances from **1**–**3**, with **3** having $W(CO)_5$ groups showing the longest, and **1** having the $Cr(CO)_5$ groups showing the shortest distances. For the tin compounds **4**–**6**, no such variation is apparent (Table 2). The angles within and subtended by the main-group octahedra are fairly constant throughout and are in each case close to the values expected for an ideal octahedron (E–E–E: 60°, 90°; M–E–E: 135°; Table 2). The angles

Table 2. Selected bond lengths [pm] and angles [°] of compounds $[Ph_4P^+]_2$·**1**−**6** (labels refer to Figure 1 throughout, with E1 on the tetragonal axis in each case)

	$[Ph_4P^+]_2$·**1**	$[Ph_4P^+]_2$·**2**	$[Ph_4P^+]_2$·**3**	$[Ph_4P^+]_2$·**4**	$[Ph_4P^+]_2$·**5**	$[Ph_4P^+]_2$·**6**
E1−E2	254.1(1)	258.0(4)	259.2(4)	293.0(1)	292.8(1)	292.8(3)
E2−E2A	252.5(2)	256.7(5)	259.2(5)	291.7(1)	290.2(1)	289.2(3)
E1−M1	242.6(2)	257.3(6)	255.7(5)	262.6(2)	271.1(3)	269.4(4)
E2−M2	239.5(2)	254.8(4)	251.8(3)	258.3(1)	273.5(1)	273.2(2)
M1−E1−E2	135.4(3)	135.3(1)	135.0(1)	135.3(1)	135.5(1)	135.7(5)
M2−E2−E2A	135.00	135.00	135.00	139.5(1)	134.5(1)	134.3(5)
M2−E2−E1	134.7(1)	134.7(1)	135.0(1)	134.6(1)	135.00	135.00
E1−E2−E2A	60.2(1)	60.2(1)	60.0(1)	60.2(1)	60.3(1)	60.4(3)
E2−E1−E2A	59.6(1)	59.7(1)	60.0(1)	59.7(1)	59.4(3)	59.2(6)
	89.3(1)	89.4(2)	90.0(2)	89.5(1)	89.00(5)	88.6(1)
E1−E2−E1A	90.7(1)	90.6(2)	90.0(2)	90.5(1)	91.0(5)	91.4(1)
E2−E2A−E2B	90.00	90.00	90.00	89.5(1)	90.00	90.00
E1−M1−C(ax)	180.0	180.0	180.0	180.0	180.0	180.0
E2−M2−C(ax)	180.0(3)	180.0(6)	180.0(1)	180.0(2)	180.0(4)	180.0(9)
E−M−C(eq)	86.7(3)−88.9(2)	87.1(7)−89.1(6)	86.0(9)−88.9(9)	87.7(2)−88.8(2)	86.3(5)−88.4(5)	87.2(6)−89.9(9)
C(ax)−M−C(eq)	91.1(2)−93.3(2)	91.0(6)−92.9(7)	91.1(9)−94.0(9)	91.2(2)−91.5(2)	91.5(5)−92.3(7)	90.1(9)−92.8(6)
C(eq)−M−C(eq)	89.0(3)−90.8(3)	89.2(9)−91.0(6)	89.0(1)−90.7(1)	89.2(3)−90.0(1)	88.7(6)−89.9(1)	86.4(5)−90.0(1)
	173.4(5)−177.8(4)	174.2(9)−177.0(6)	175.9(2)−177.7(2)	175.3(3)−177.6(4)	175.3(9)−176.8(9(	174.4(9)- 179.9(9)
M1−C(ax)−O(ax)	180.0	180.0	180.0	180.0	180.0	180.0
M2−C(ax)−O(ax)	180.0(9)	180.0(9)	180.0(1)	180.0(5)	180.0(1)	180.0(9)
M−C(eq)−O(eq)	176.9(7)−179.8(6)	174.2(9)−178.1(9)	176.2(3)−178.0(3)	178.1(5)−179.3(5)	177.4(9)−179.2(9)	176.7(9)−179.5(9)

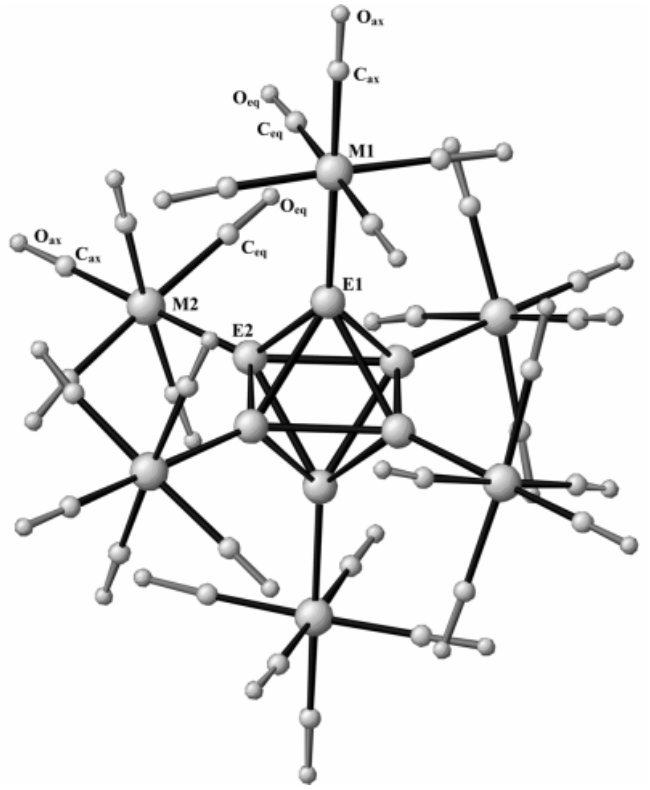

Figure 1. Structure of **2** as a representative of the architecture of **1**−**6**; labels refer to Table 2; the tetragonal axis is vertical in Figure 1, with E1 lying on this axis

describing the geometry of the $M(CO)_5$ fragments (Table 2) indicate a slight umbrella effect with the equatorial carbonyl groups bending towards the main-group centre. An overview of the geometric parameters characterising the $[E_6]^{2-}$ core of the clusters given in Table 2 makes it clear that neither the kind of the protective groups $M(CO)_5$ (M = Cr, Mo, W), nor the specific crystal environment, have a strong influence on the structure of the cluster core. It appears therefore that the observed geometry corresponds to a well-defined energy minimum on the corresponding hypersurface.

The idealised *closo* octahedral structure of the $[E_6]^{2-}$ core should therefore also characterise the structure of the compounds in solution. The pattern of $\tilde{\nu}$(CO) infrared bands observed for **1**−**6** (Table 3) is simple enough to substantiate this expectation. With two $M(CO)_5$ groups in slightly different chemical environments, a maximum of six absorptions should be expected. A maximum of five absorptions is observed (Table 3), and only four bands are apparent in most cases.

Table 3. $\tilde{\nu}$(CO) − IR spectroscopic data of compounds $[Ph_4P^+]_2$·**1**−**6**

	$\tilde{\nu}$(CO) − IR [cm^{-1}]				
$[Ph_4P^+]_2$·**1**[a]	–	2043s	2010w	1951vs	1910s
$[Ph_4P^+]_2$·**2**[a]	–	2056s	2029m	1957vs	1907vs
$[Ph_4P^+]_2$·**3**[a]	–	2056s	2031m	1952vs	1910s
$[Ph_4P^+]_2$·**4**[b]	2052m	2037s	–	1943vs	1912vs
$[Ph_4P^+]_2$·**5**[b]	2070w	2052s	2013w	1951vs	1907vs
$[Ph_4P^+]_2$·**6**[b]	2068w	2052s	2017m	1945vs	1905vs

[a] DMA. − [b] THF.

This indicates that the high symmetry found in the anions in the solid state is also preserved in solution. A more direct indication of a cluster geometry that is octahedral on average, comes from NMR spectroscopy. The ^{119}Sn resonances of **4**−**6** (Table 4) show clear tin satellites in each case, with coupling constants of approximately 1800 Hz, characteristic of tin−tin contacts.[24] The integral ratio of the main signal to the satellites is as expected for an arrangement in which the observed tin nucleus is surrounded by four other nuclei, each of them in an abundance of 7.6% (calculated: 30.4%; observed 28%).[25] The ^{119}Sn NMR spectrum of $[Ph_4P^+]_2$·**6**

shows ^{183}W coupling with $^1J_{W-Sn} = 700$ Hz for the main signal, as well as for the satellites. In agreement with the overall octahedral geometry, there is only one ^{13}C resonance for the equatorial CO groups of compounds **1−6**, and one for the axial carbonyl groups, wherever these could be measured (solubility) (Table 4).

The $[E_6]^{2-}$ octahedra acting as the ligand core in compounds **1−6** are electron-precise *closo* clusters.[15,16] As a result of a low-lying HOMO and a high-energy LUMO, these clusters should be difficult to oxidise and reduce. Cyclic voltammetry reveals (Table 5) that despite the charge of −2 on these clusters, their oxidation occurs only at approximately +0.3 V (vs. SCE). This oxidation is reversible in some cases (Table 5). It thus follows that removing an electron from the filled t_{1u} HOMO does not induce a strong distortion of the cluster. Further irreversible oxidation of the cluster core is observed in the range up to approximately +0.8 V (vs. SCE) (Table 5). At higher potentials, the $M(CO)_5$ groups are oxidised. The peaks corresponding to an oxidation of the $M(CO)_5$ groups are roughly six times larger than the peaks that correspond to electron-transfer processes involving the cluster core. Polarograms also show an approximate 1:6 ratio of the corresponding step heights. This must mean that electron transfer involving the cluster core includes the whole $[E_6]^{2-}$ entity and not just one individual main-group centre, while electron transfer involving the $M(CO)_5$ entities involves each such group individually. Reduction of compounds **1−6** is irreversible throughout and occurs between −0.6 and −0.9 V (vs. SCE) (Table 5). Reduction of the $M(CO)_5$ entities is observed from approximately −1.4 V (vs. SCE) towards lower potentials and is also irreversible (Table 5).

The reversible oxidation of the cluster core documented by the cyclovoltammetric experiments would suggest that the cluster dianions could also be oxidised to the monoanions by chemical means. However, it was found that mild oxidants (sulfur, propylene sulfide, Fc^+), applied in solvents such as CS_2, DMA, THF, or mixtures of these, leave the dianions unchanged (IR control) for hours. Strong oxidants such as I_2 and tetrabromoorthoquinone lead to fragmentation of the clusters. The sodium salts of the cluster dianions are also stable against chemical reduction: Their THF solutions may be in contact with KC_8 without any sign of change, even after several days.

The cyclovoltammetric data indicate that the HOMO−LUMO separation within the clusters should be roughly 1.5 eV. Hence, if electronic HOMO−LUMO transitions were allowed, these would be expected to occur in the

Table 4. ^1H, $^{31}P\{^1H\}$, and $^{13}C\{^1H\}$ NMR spectroscopic data of compounds $[Ph_4P^+]_2$·**1−6**

	^1H $H_{arom.}$[c]	$^{31}P\{^1H\}$	$^{119}Sn\{^1H\}$	$^{13}C\{^1H\}$[d] CO_{ax}	CO_{eq}	C_{para}	C_{ortho}	C_{meta}	C_{ipso}
$[Ph_4P^+]_2$·**1**[a]	8.01−7.67	23.6	–	222.2	217.0	136.2	135.4	131.3	118.8
$[Ph_4P^+]_2$·**2**[a]	7.97−7.69	23.6	–	–	206.4	135.2	134.3	130.3	117.5
$[Ph_4P^+]_2$·**3**[a]	7.97−7.69	23.6	–	–	197.6	135.2	134.4	130.3	117.6
$[Ph_4P^+]_2$·**4**[b]	7.87	24.3	508 ($^1J_{Sn-Sn}$ = 1848 Hz)	–	218.0	136.4	135.6	131.4	118.9
$[Ph_4P^+]_2$·**5**[b]	7.87	26.3	561 ($^1J_{Sn-Sn}$ = 1780 Hz)	–	–	136.2	135.5	131.2	188.8
$[Ph_4P^+]_2$·**6**[b]	8.03−7.87	24.3	198 ($^1J_{Sn-Sn}$ = 1803 Hz, $^1J_{W-Sn}$ = 700 Hz)	204.7	198.8	136.4	135.7	131.4	119.0

[a] $[D_6]$DMSO. − [b] $[D_6]$acetone. − [c] Unresolved multiplets. − [d] C_{para} [d, $^4J(^{31}P,^{13}C)$ = 3 Hz]; C_{ortho} [d, $^2J(^{31}P,^{13}C)$ = 10 Hz]; C_{meta} [d, $^3J(^{31}P,^{13}C)$ = 13 Hz]; C_{ipso} [d, $^1J(^{31}P,^{13}C)$ = 89 Hz]; $[Ph_4P^+]$.

Table 5. Analytical data of compounds $[Ph_4P^+]_2$·**1−6**

	M.p. [°C]	UV/nm (THF/DMA) λ_{max} (ε [l mol^{-1} cm^{-1}])	Empirical formula (mol. mass)	Elemental analysis	CV (CH_3CN)[a] [V]
$[Ph_4P^+]_2$·**1**	104−105 (dec.)	276 (12000); 301 (12000); 365 (3000)	$C_{78}H_{40}O_{30}P_2Cr_6Ge_6$ (2266.62)	calcd. C 41.33 H 1.78 found C 41.27 H 2.01	Ox: +0.34rev., +0.81, + 1.12 Red.: −0.92, −1.54, −1.75, −1.94
$[Ph_4P^+]_2$·**2**	160−163 (dec.)	298 (12400); 325 (12000); 377 (6400)	$C_{78}H_{40}O_{30}P_2Mo_6Ge_6$ (2530.27)	calcd. C 37.03 H 1.59 found C 37.20 H 1.92	Ox.: +0.29rev., +0.70, +0.82, +1.08 Red.: −1.44, −1.74, −1.93
$[Ph_4P^+]_2$·**3**	228−229 (dec.)	276 (16000); 329 (4500); 375 (3000)	$C_{78}H_{40}O_{30}P_2W_6Ge_6$ (3057.81)	calcd. C 30.64 H 1.32 found C 28.69 H 1.72	Ox.: +0.62, +0.86, +1.10 Red.: −0.90, −1.44, −1.62, −1.93
$[Ph_4P^+]_2$·**4**	207−208 (dec.)	329 (30800); 392 (7000)	$C_{78}H_{40}O_{30}P_2Cr_6Sn_6$ (2543.22)	calcd. C 37.66 H 1.85 found C 38.00 H 2.08	Ox.:[b] +0.39rev., +0.69, +0.83, +1.01, +1.32 Red.:[b] −0.60, −1.40, −1.48
$[Ph_4P^+]_2$·**5**	184−186 (dec.)	295 (36000); 328 (31000); 404 (12000)	$C_{78}H_{40}O_{30}P_2Mo_6Sn_6$ (2806.88)	calcd. C 33.38 H 1.44 found C 32.67 H 1.93	Ox.: +0.33, +0.48, +0.67, +0.81, +1.10 Red.: −1.39, −1.89
$[Ph_4P^+]_2$·**6**	200−201 (dec.)	295 (33000); 320 (30000); 381 (10000); 423 (8000)	$C_{78}H_{40}O_{30}P_2W_6Sn_6$ (3334.34)	calcd. C 28.10 H 1.21 found C 27.76 H 1.65	Ox.: +0.24, +0.40, +0.55, +0.87, +1.11 Red.: −1.27, −1.94

[a] Potentials were measured vs. SCE with the exception of $[Ph_4P^+]_2$·**4** (see footnote[b]). The working electrode was a glassy-carbon electrode in each case, with a platinum wire used as the counter electrode. Redox processes were judged to be reversible if the separation of their anodic and cathodic peaks was similar to the one observed for the Fc/Fc^+ redox couple in the same experiment. A square-root dependence of peak height on scan speed was taken as the second criterion. The data given for the other electrode processes refer to peak potentials E_P^R or E_P^C throughout. − [b] The potentials refer to a platinum wire as the reference electrode and are thus on a deliberate absolute scale. Whenever an SCE electrode was immersed into the solution, the compound was found to disintegrate.

visible range. MO analysis of the cluster core on the other hand reveals that these transitions are symmetry-forbidden since the HOMO has t_{1u} symmetry and the LUMO has t_{2u} symmetry. The transition from the HOMO (t_{1u}) to the LUMO+1 (t_{1g}) would be symmetry-allowed. The energy difference between the corresponding orbitals is however quite large, and owing to the shape of the orbitals, the transition moment should be small. In agreement with this, UV/Vis spectra of the $[Ph_4P]$ salts **1**−**6** (Table 5) do not show a spectroscopic pattern that could be assigned to transitions within the cluster core. The high-energy absorptions above 350 nm are characteristic of $M(CO)_5$ derivatives as a whole (see for instance ref.[21]); the lower energy absorptions at approximately 400 nm are interpreted as LMCT absorptions. In agreement with germanium having a higher electronegativity than tin, these CT bands occur at higher energy for the germanium compounds than for the tin analogues (Table 5).

Experimental Section

General: All manipulations were carried out under argon by means of standard Schlenk techniques at 20 °C unless otherwise mentioned. All solvents were dried by standard methods, and distilled under argon. $[D_6]$DMSO and $[D_6]$acetone used for the NMR spectroscopic measurements were degassed by three successive "freeze-pump-thaw" cycles and dried with 4 Å molecular sieves. Silica gel (Kieselgel z. A. 0.06−0.2 mm, J. T. Baker Chemicals B. V.) used for chromatography and Kieselgur (Kieselgur, gereinigt, geglüht, Erg. B.6, Riedel-de Haën AG) used for filtration were degassed at 1 mbar at 130 °C for 12 h and saturated with argon. − NMR: Bruker Avance DPX 200 at 200.13 MHz (^{1}H), 50.323 MHz (^{13}C{^{1}H}), 81.015 MHz (^{31}P{^{1}H}), 74.631 MHz (^{119}Sn{^{1}H}); chemical shifts (δ) in ppm relative to $[D_6]$DMSO (^{1}H: δ = 2.50; ^{13}C: δ = 39.4) and $[D_6]$acetone (^{1}H: δ = 2.05; ^{13}C: δ = 206.2) as internal standards and to 85% H_3PO_4 (^{31}P: δ = 0) and $(CH_3)_4Sn$ (^{119}Sn: δ = 0) as external standards, respectively. − IR: Bruker FT-IR IFS-66; CaF_2 cells. − UV/Vis/NIR: Perkin−Elmer Lambda 19; cells (0.2 cm; Hellma 110 suprasil). − Cyclic voltammetry: Methrom "Universal Meß- und Titriergefäß", Methrom GC electrode RDE 628, platinum electrode, SCE electrode, Princeton Applied Research Potentiostat Model 273, 10^{-3} M in 0.1 M nBu$_4$NPF$_6$/CH_3CN. − Elemental analysis: Microanalytical laboratory of the Organisch-Chemisches Institut, Universität Heidelberg. − Melting points: Gallenkamp MFB-595 010; the values are not corrected.

Preparation of $[Ph_4P]_2[\{(OC)_5M\}_6Ge_6]$, $[Ph_4P^+]_2$·1, $[Ph_4P^+]_2$·2, $[Ph_4P^+]_2$·3 (M = Cr, Mo, W)

Method 1, the "bipy Method" (Suitable for the Preparation of $[Ph_4P^+]_2$·1−3): To a stirred orange solution of $Na_2[M_2(CO)_{10}]$[18] (M = Cr: 430 mg, 1 mmol; M = Mo: 518 mg, 1 mmol; M = W: 694 mg, 1 mmol) in THF (50 mL), solid GeI_2 (326 mg, 1 mmol) and solid 2,2′-bipyridine (156 mg, 1 mmol) were added in one portion. After stirring for 30 min, the deep red solution was filtered through Kieselgur (3 cm, Ø = 3 cm), concentrated in vacuo (3 mL) and purified by chromatography on silica gel (15 cm, Ø = 3 cm; THF). With THF as the eluent all by-products could be removed.[2,17,22] After elution with ethanol, the solutions of the sodium salts of **1**, **2**, and **3**, respectively, were obtained, which were reduced to 10 mL in vacuo. Addition of solid $[Ph_4P]Cl$ (750 mg, 2 mmol) led to the red-brown $[Ph_4P]$ salts of **1**, **2**, and **3**, which were separated from the mother liquor by filtration, washed with ethanol (2 × 5 mL) and diethyl ether (2 × 5 mL), and dried in vacuo. Yields: $[Ph_4P^+]_2$·**1**: 43 mg, 0.02 mmol, 11%; $[Ph_4P^+]_2$·**2**: 42 mg, 0.02 mmol, 9% $[Ph_4P^+]_2$·**3**: 50 mg, 0.02 mmol, 9% (with respect to GeI_2).

Method 2, Reduction with $K_2[M_2(CO)_{10}]$ (Suitable for the Preparation of $[Ph_4P^+]_2$·2, $[Ph_4P^+]_2$·3): KC_8 [811 mg, 6 mmol, freshly prepared by dry heating of graphite powder (577 mg, 48 mmol) with potassium (235 mg, 6 mmol) by a heat gun (650 °C) in a Schlenk tube under vacuum] and $M(CO)_6$ (M = Mo: 6 mmol = 1.58 g, M = W: 2.11 g, 6 mmol) in THF (50 mL) were stirred for 12 h at 20 °C, during which time CO evolution had ceased. After this period of time, solid GeI_2 (326 mg, 1 mmol) was added to the dark green heterogeneous mixture, causing a colour change to deep brown. After stirring for 1 h, the reaction mixture was filtered through Kieselgur (3 cm, Ø = 3 cm) and concentrated in vacuo (3 mL). Further workup was carried out as in Method 1. Yields: $[Ph_4P^+]_2$·**2**: 220 mg, 0.08 mmol, 47% $[Ph_4P^+]_2$·**3**: 320 mg, 0.10 mmol, 60% (with respect to GeI_2).

Method 3, Reduction of Tetraiododigermanates by Decacarbonyldimetallate (Suitable for the Preparation of $[Ph_4P^+]_2$·1, $[Ph_4P^+]_2$·3): To a solution of $Na_2[\{(OC)_5M\}I_2Ge-GeI_2\{M(CO)_5\}]$[17] (M = Cr, W) in THF (30 mL), a solution of $Na_2[M_2(CO)_{10}]$[18] in THF (30 mL) was added in 10-mL portions during a period of 3 h. The colour of the solution gradually turned to red-brown. Further workup was carried out as in Method 1. Yields: $[Ph_4P^+]_2$·**1**: 151 mg, 0.07 mmol, 40%; $[Ph_4P^+]_2$·**3**: 310 mg, 0.10 mmol, 60% (with respect to GeI_2).

Method 4, Reduction of Tetraiododigermanates with KC_8 (Suitable for the Preparation of $[Ph_4P^+]_2$·1, $[Ph_4P^+]_2$·3): To solid KC_8 [540 mg, 4 mmol; freshly prepared from graphite powder (384 mg, 32 mmol) and potassium (156 mg, 4 mmol) as above], a solution of $Na_2[\{(OC)_5M\}I_2Ge-GeI_2\{M(CO)_5\}]$[17] (M = Cr, W) in THF (50 mL) was added and stirred for 1 h. Further workup was carried out as in Method 1. Yields: $[Ph_4P^+]_2$·**1**: 164 mg, 0.07 mmol, 42%; $[Ph_4P^+]_2$·**3**: 306 mg, 0.10 mmol, 60% (with respect to GeI_2). Single crystals suitable for X-ray structure analysis were obtained by layering concentrated DMA solutions of $[Ph_4P^+]_2$·**1**, $[Ph_4P^+]_2$·**2**, and $[Ph_4P^+]_2$·**3** with ethanol.

Preparation of $[Ph_4P]_2[\{(OC)_5M\}_6Sn_6]$, $[Ph_4P^+]_2$·4 (M = Cr), $[Ph_4P^+]_2$·6 (M = W): To a stirred orange solution of $Na_2[M_2(CO)_{10}]$[18] (M = Cr: 430 mg, 1 mmol; M = W: 694 mg, 1 mmol) in THF (50 mL), solid $SnCl_2$ (190 mg, 1 mmol) was added in one portion. The orange solution turned deep red immediately. After stirring for 30 min, the reaction mixture was filtered through Kieselgur (3 cm, Ø = 3 cm). The resulting red solution was concentrated in vacuo (3 mL) and purified by chromatography on silica gel (15 cm, Ø = 3 cm; THF). A mixture of THF/ethanol (15:1) was used until the elute was colourless. A red band remained on top of the column and could be eluted with ethanol. $[Na^+]_2$·**4** and $[Na^+]_2$·**6** were obtained as deep red ethanolic solutions, which were concentrated to 10 mL in vacuo. Addition of solid $[Ph_4P]Cl$ (750 mg, 1 mmol) led to the corresponding deep red $[Ph_4P]$ salts of **4** and **6**, respectively, which precipitated immediately. The solids were separated from the mother liquor by filtration, washed with ethanol (2 × 5 mL), diethyl ether (2 × 10 mL), and dried in vacuo. Yields: $[Ph_4P^+]_2$·**4**: 46 mg, 0.02 mmol, 11%; $[Ph_4P^+]_2$·**6**: 50 mg, 0.02 mmol, 9% (with respect to $SnCl_2$). For growing single crystals of $[Ph_4P^+]_2$·**4** and $[Ph_4P^+]_2$·**6**, the deep-red solids were dissolved in

Table 6. Crystal structure data of compounds $[Ph_4P^+]_2$·**1**−**6**

Compound	$[Ph_4P^+]_2$·**1**	$[Ph_4P^+]_2$·**2**	$[Ph_4P^+]_2$·**3**	$[Ph_4P^+]_2$·**4**·thf	$[Ph_4P^+]_2$·**5**	$[Ph_4P^+]_2$·**6**
Empirical formula	$C_{78}H_{40}Cr_6Ge_6O_{30}P_2$	$C_{78}H_{40}Ge_6Mo_6O_{30}P_2$	$C_{78}H_{40}Ge_6O_{30}P_2W_6$	$C_{82}H_{40}Cr_6O_{31}P_2Sn_6$	$C_{78}H_{40}Mo_6O_{30}P_2Sn_6$	$C_{78}H_{40}O_{30}P_2Sn_6W_6$
Molecular mass [g/mol]	2266.56	2530.27	3057.81	2607.22	2806.88	3334.34
Crystal dimension [mm]	0.20·0.20·0.25	0.15·0.15·0.15	0.10·0.10·0.10	0.35·0.35·0.25	0.30·0.30·0.20	0.35·0.35·0.25
Crystal system	tetragonal	tetragonal	tetragonal	tetragonal	tetragonal	tetragonal
space group (no.)	*P4/nnc* (126)	*P4/nnc* (126)	*I4/mmm* (139)	*I4/m* (87)	*I4/mmm* (139)	*I4/mmm* (139)
a [pm]	1462.1(6)	1514.4(3)	1499.8(2)	1294.7(1)	1594.5(1)	1573.3(1)
b [pm]	1462.1(6)	1514.4(3)	1499.8(2)	1294.7(1)	1594.5(1)	1573.1(1)
c [pm]	1970.0(6)	1971.3(5)	1971.8(4)	2815.7(5)	1912.2(2)	1897.3(1)
Cell volume [10^6pm^3]	4211(3)	4521(2)	4435(1)	4720(1)	4862(1)	4696(1)
Molecular units/cell	2	2	2	2	2	2
Density (calculated) [g cm^{-3}]	1.787	1.859	2.787	1.835	1.890	2.329
Temperature [K]	200	200	200	200	210	200
No. of reflns. for cell parameter refinement	32	28		41	25	31
Scan range	$4.1° \le 2\Theta \le 50°$	$3.4° \le 2\Theta \le 51°$	$3.4° \le 2\Theta \le 52°$	$3.5° \le 2\Theta \le 49°$	$5.1° \le 2\Theta \le 54°$	$4.3° \le 2\Theta \le 54°$
Scan speed (ω) [° min^{-1}]	10	8		10	10	6
Integration time [s/frame]			10			
No. of rflns. measured	4251	4101	12416	2738	2948	2809
No. of unique rflns.	1864	2117	1284	2009	1548	1486
No. of rflns. observed ($\ge 2\sigma$)	1067	807	986	1719	1036	1016
No. of parameters refined	144	132	97	159	134	109
residual electron density [·10^{-6} e pm^{-3}]	0.85/−0.91	1.63/−1.56	4.00/−1.60	0.89/−0.44	0.49/−0.83	1.74/−2.30
R_1/R_w [%] (refinement on F^2)	4.2/13.4	8.9/33.6	7.0/18.9	3.3/9.3	5.3/12.9	5.3/14.8

THF (5 mL) and layered with ethanol (20 mL). Within one week at 20 °C, deep-red crystals suitable for X-ray analysis were obtained.

Preparation of $[Ph_4P]_2[\{(OC)_5Mo\}_6Sn_6]$, $[Ph_4P^+]_2$·5: To a stirred ethanolic solution (50 mL) of $Na_2[Mo_2(CO)_{10}]$[18] (518 mg, 1 mmol), solid $SnCl_2$ (190 mg, 1 mmol) was added in one portion. After 30 min of stirring, the deep red solution was filtered through Kieselgur (3 cm, Ø = 3 cm), reduced to a volume of 10 mL in vacuo. Upon addition of solid $[Ph_4P]Cl$ (750 mg, 1 mmol), the red $[Ph_4P]$ salt of **5** precipitated immediately and was separated from the mother liquor by filtration. After washing the red solid with ethanol (2 × 5 mL) and diethyl ether (2 × 10 mL), the residue was dried in vacuo. Yield: $[Ph_4P^+]_2$·**5**: 171 mg, 0.06 mmol, 36% (with respect to $SnCl_2$). For growing single crystals of $[Ph_4P^+]_2$·**5**, the red solid was dissolved in THF (5 mL) and layered with ethanol (20 mL). Within one week at 20 °C, red crystals suitable for X-ray analysis were obtained.

X-ray Structure Determinations: The measurements for $[Ph_4P^+]_2$·**1**, **2**, **4**, **5**, **6** were carried out with a Siemens P4 four-circle diffractometer. Data for $[Ph_4P^+]_2$·**3** were collected with a Nonius Kappa CCD diffractometer, all using Mo-K_α radiation. In the case of the data collection with the Siemens P4 four-circle diffractometer, the intensities of three check reflections (measured every 100 reflections) remained constant throughout, thus indicating crystal and electronic stability. The data collected using a scintillation counter measuring device (Siemens P4) were corrected as usual including experimental absorption correction. The data from the CCD device (Nonius Kappa CCD) were processed by the standard Nonius software.[26] All calculations were performed using the SHELXT PLUS software package. Structures were solved by direct methods with the SHELXS-86 program and refined with the SHELXL-93 program.[27−29] The program XPMA[30] and WinRay32[31] were used for graphical handling of the data. The structures were refined in fully or partially anisotropic models by full-matrix least-squares calculations. Hydrogen atoms were introduced at calculated positions. The data for the structure determinations is presented in Table 6. Crystallographic data for the structures reported in this paper (except for $[Ph_4P^+]_2$·**1**: CSD-408093[2]) have been deposited with the Cambridge Crystallographic Data Centre as supplementary publications no. CCDC-149568 ($[Ph_4P^+]_2$·**2**), -149565 ($[Ph_4P^+]_2$·**3**), -149564 ($[Ph_4P^+]_2$·**4**), -149566 ($[Ph_4P^+]_2$·**5**), and -149567 ($[Ph_4P^+]_2$·**6**). Copies of the data can be obtained free of charge on application to CCDC, 12 Union Road, Cambridge CB2 1EZ, UK [Fax: (internat.) + 44-1223/336-033; E-mail: deposit@ccdc.cam.ac.uk].

[1] B. Schiemenz, G. Huttner, *Angew. Chem.* **1993**, *105*, 295−296; *Angew. Chem. Int. Ed. Engl.* **1993**, *32*, 297−298.

[2] P. Kircher, G. Huttner, K. Heinze, G. Renner, *Angew. Chem.* **1998**, *110*, 1754−1755; *Angew. Chem. Int. Ed.* **1998**, *37*, 1664−1665.

[3] J. D. Corbett, *Angew. Chem.* **2000**, *112*, 682−704; *Angew. Chem. Int. Ed.* **2000**, *39*, 670−690.

[4] R. W. Rudolph, W. L. Wilson, R. C. Taylor, *J. Am. Chem. Soc.* **1981**, *103*, 2480−2481.

[5] S. C. Critchlow, J. D. Corbett, *J. Chem. Soc., Chem. Commun.* **1981**, 236−237.

[6] C. H. E. Belin, J. D. Corbett, A. Cisar, *J. Am. Chem. Soc.* **1977**, *99*, 7163−7169.

[7] C. Belin, H. Mercier, V. Angilella, *New J. Chem.* **1991**, *15*, 931−938.

[8] V. Queneau, S. C. Sevov, *Angew. Chem.* **1997**, *109*, 1818−1820; *Angew. Chem. Int. Ed. Engl.* **1997**, *36*, 1754−1756.

[9] T. F. Fässler, M. Hunziker, *Inorg. Chem.* **1994**, *33*, 5380−5381.

[10] C. Downie, Z. Tang, A. M. Guloy, *Angew. Chem.* **2000**, *112*, 346−348; *Angew. Chem. Int. Ed.* **2000**, *39*, 337−340.

[11] D. Kummer, L. Diehl, *Angew. Chem.* **1970**, *82*, 881−882; *Angew. Chem. Int. Ed. Engl.* **1970**, *9*, 895−896.

[12] H. G. von Schnering, *Angew. Chem.* **1981**, *93*, 44−63; *Angew. Chem. Int. Ed. Engl.* **1981**, *20*, 33−52.

[13] An organic derivative containing a trigonal prismatic Ge_6 core of heteroprismane-type structure has been reported: A. Sekiguchi, C. Kabuto, H. Sakurai, *Angew. Chem.* **1989**, *101*, 97−98; *Angew. Chem. Int. Ed. Engl.* **1989**, *28*, 55−56.

[14] A Ge_6 arrangement, possibly octahedral in shape, is inferred for the series of gas-phase clusters $[Ge_6Cl_n]^{m-}$: P. Jackson, K. J. Fischer, G. E. Gadd, I. G. Dance, D. R. Smith, G. D. Willett, *Int. J. Mass Spectrom. Ion Process* **1997**, *164*, 45−69.

[15] K. Wade, *Adv. Inorg. Chem. Radiochem.* **1976**, *18*, 1−66.

[16] D. M. P. Mingos, R. L. Johnston, *Struct. Bond.* **1987**, *68*, 29−87.

[17] G. Renner, P. Kircher, G. Huttner, P. Rutsch, *Eur. J. Inorg. Chem.* **2000**, 879−887.
[18] E. Lindner, H. Behrens, S. Birkle, *J. Organomet. Chem.* **1968**, *15*, 165−175.
[19] L. B. Handy, J. K. Ruff, L. F. Dahl, *J. Am. Chem. Soc.* **1970**, *92*, 7312−7326.
[20] This is in contrast to the idea put forward in ref.[2] that bipy is essential as an electron-transfer reagent in the synthesis of **1**.
[21] P. Kircher, G. Huttner, K. Heinze, *J. Organomet. Chem.* **1998**, *562*, 217−227.
[22] P. Kircher, G. Huttner, B. Schiemenz, K. Heinze, L. Zsolnai, O. Walter, A. Jacobi, A. Driess, *Chem. Ber./Recueil* **1997**, *130*, 687−699.
[23] P. Kircher, G. Huttner, K. Heinze, B. Schiemenz, L. Zsolnai, M. Büchner, A. Driess, *Eur. J. Inorg. Chem.* **1998**, 703−720.
[24] R. W. Rudolph, W. L. Wilson, F. Parker, R. C. Taylor, D. C. Young, *J. Am. Chem. Soc.* **1978**, *100*, 4629−4630.
[25] In comparing the integrals of the peaks it is assumed that in agreement with the symmetry of the compound, the relaxation times of the nuclei are equal and therefore the integrals are affected by the measurement technique to the same extent.
[26] Collect datacollection software, Nonius, **1998**; http://www.nonius.com
[27] G. M. Sheldrick, *SHELXS-86 − Program for Crystal Structure Solution*, University of Göttingen, **1986**; http://www.shelx.uni-ac.gwdg.de/shelx/index.html
[28] G. M. Sheldrick, *SHELXL-93 − Program for Crystal Structure Refinement*, University of Göttingen, **1993**; http://www.shelx.uni-ac.gwdg.de/shelx/index.html
[29] *International Tables for X-ray Crystallography*, Kynoch-Press, Birmingham, **1974**, vol. 4.
[30] L. Zsolnai, G. Huttner, *XPMA*, University of Heidelberg, **1998**; http://www.rzuser.uni-heidelberg.de/~il1/laszlo/xpm.html
[31] R. Soltek, *WinRay32*, University of Heidelberg, **2000**; http://www.uni-heidelberg.de/institute/fak12/AC/huttner/frame/frame_soft.html

Received September 18, 2000
[I00348]